Understanding Effect of Wall Structure on the Hydrothermal Stability of Mesostructured Silica SBA-15

Fuqiang Zhang, Yan Yan, Haifeng Yang, Yan Meng, Chengzhong Yu, Bo Tu, and Dongyuan Zhao*

Department of Chemistry, Molecular Catalysis and Innovative Materials Laboratory, Fudan University, Shanghai 200433, People's Republic of China

Received: November 24, 2004; In Final Form: March 5, 2005

Mesostructured silica SBA-15 materials with different structural parameters, such as pore size, pore volume, and wall thickness, etc., were prepared by varying the postsynthesis hydrothermal treatment temperature and adding inorganic salts. The hydrothermal stabilities of these materials in steam (100% water vapor) were systematically investigated using a variety of techniques including powder X-ray diffraction, transmission electron microscopy, nitrogen sorption, and ^{29}Si solid-state NMR. The effect of the pore size, microporosity or mesoporosity, and wall thickness on the stability was discussed. The results show that all of the SBA-15 materials have a good hydrothermal stability under steam of 600 °C for at least 24 h. N_2 sorption measurements show that the Brumauer−Emmett−Teller surface area of SBA-15 materials is decreased by about 62% after treatment under steam at 600 °C for 24 h. The materials with thicker walls and more micropores show relatively better hydrothermal stability in steam of 600 °C. Interestingly, we found that the microporosity of the mesostructured silica SBA-15 is a very important factor for the hydrothermal stability. To the materials with more micropores, the recombination of Si−O−Si bonds during the high-temperature steam treatment may not cause direct destruction to the wall structure. As a result, SBA-15 materials with more micropores show better stability in pure steam of 600 °C. Nevertheless, these materials are easily destroyed in steam of 800 °C for 6 h. Two methods to effectively improve the hydrothermal stability are introduced here: one is a high-temperature treatment, and another is a carbon-propping thermal treatment. Thermal treatment at 900 °C can enhance the polymerization degree of ≡Si−O−Si≡ bonds and effectively improve the hydrothermal stability of these SBA-15 materials in 800 °C steam for 12 h. But, this approach will cause very serious shrinkage of the mesopores, resulting in smaller pore diameter and low surface area. A carbon-propping thermal treating method was employed to enhance the polymerization of ≡Si−O−Si≡ bonds and minimize the serious shrinkage of mesopores at the same time. It was demonstrated to be an effective method that can greatly improve the hydrothermal stability of SBA-15 materials in 800 °C steam for 12 h. Furthermore, the SBA-15 materials obtained by using the carbon-propping method possess larger pores and higher surface area after the steam treatment at 800 °C compared to the materials from the direct thermal treatment method after the steam treatment.

Introduction

Since its first discovery in 1992,[1,2] highly ordered mesoporous silicate materials with high surface area, large pore size, and large pore volume have attracted great interest for their potentially wide applications in catalysis, adsorption, separation, and ion exchange, etc. Up to now, a variety of highly ordered mesoporous silica materials (M41S,[1,2] SBA,[3,4] MSU,[5] FDU,[6,7] HMS,[8,9] and KIT,[10] etc.) have been successfully synthesized. Functional groups or metal oxides with catalytic activity can be easily incorporated onto the pore walls of mesoporous silica materials due to the numerous silanols on the pore walls.[9,11−13] It has been reported that mesoporous silica materials incorporated with transition metals show outstanding catalytic activities in the conversion of a large molecule.[9,14−16]

However, mesoporous silica materials have not been widely used as catalysts or catalyst supports in industry yet. This is mainly because of the poor hydrothermal stability of mesoporous silicates under the critical conditions of industrial applications, where the materials are often exposed to water steam at 600−800 °C or to boiling water. The hydrothermal stability in pure steam at 600−800 °C is of special importance in industrial applications such as catalytic cracking. MCM-41 and MCM-48 materials are easily destroyed in boiling water and steam as a result of the fast hydrolysis of the relatively thin amorphous silica walls.[10,17−19] Due to their poor hydrothermal stability, numerous efforts have been carried out to improve the hydrothermal stability of mesoporous materials.[19−25] For example, the addition of inorganic salts (such as KCl, NaCl, and NaF, etc.) during the crystallization process or postsynthesis hydrothermal process has been demonstrated to be an effective approach to improve the hydrothermal stability of such materials in boiling water.[19−21,26,27] These strategies were shown to increase either the wall thickness or the degree of polymerization of the silica wall. Incorporation of metal oxides, such as aluminum and vanadium oxides, was also demonstrated to be an effective method to improve the hydrothermal stability.[28,29] To date, the investigations on the "hydrothermal stability" of

* To whom correspondence should be addressed. Telephone: 86-21-65642036. Fax: 86-21-6564-1740. E-mail: dyzhao@fudan.edu.cn.

10.1021/jp044632+ CCC: $30.25
Published on Web 04/02/2005

mesoporous materials are most carried out in boiling water and are seldom reported in pure steam at 600−800 °C. The hydrothermal stability under steam conditions is, however, of special importance to their catalytic applications in industry.

Mesoporous silica SBA-15 materials show great advantages as catalyst supports and adsorbents for large molecules because of their large and tunable pore diameter (5−30 nm), high surface area (600−1000 m^2/g), and large pore volume (up to 2.2 cm^3/g). Unlike the M41S (MCM-41 and MCM-48) materials, which were synthesized by using an ionic surfactant such as CTAB (cetyltrimethylammonium bromide) as a template in basic media, SBA-15 materials are prepared using amphiphilic nonionic triblock copolymer P123 ($EO_{20}PO_{70}EO_{20}$) as a template in acidic media.[3] The mesoporous silica materials prepared using the block copolymers possess larger pores and thicker pore walls compared to those prepared using ionic surfactants. The pore diameter of SBA-15 materials can be easily tuned by varying the temperature of postsynthesis hydrothermal restructuring procedures. The outstanding properties of SBA-15 will expand the application fields of mesoporous materials.

The pore wall structure of SBA-15 materials differs greatly from those of MCM-41 materials. In as-synthesized SBA-15, a considerable amount of the hydrophilic poly(ethylene oxides) (PEO) blocks are embedded in the silica walls, which may generate micropores after calcination. Recently, several detailed structure elucidation studies of SBA-15 have been reported, wherein the existence of micropores within the pore walls of SBA-15 was confirmed.[30−33] The micropores within the pore walls of SBA-15 can be controlled by adding salts and varying temperature during the crystallization process.[34] Due to the different structures, the strategies employed to improve the hydrothermal stability of MCM-41 are no more suitable to SBA-15.

However, to the best of our knowledge, there has been no detailed study of the hydrothermal stability of silica SBA-15 for a better understanding of the crucial structural parameters that influence the hydrothermal stability. Furthermore, the hydrothermal stability of mesoporous SBA-15 in pure steam at 600−800 °C, to which the catalysts are often exposed under industrial conditions, was seldom described in the literature.[35] In this paper, we report the results of a detailed and systematic investigation of the effect of the pore wall structure, of samples prepared by varying the synthesis conditions, on the hydrothermal stability of pure silica SBA-15 in pure steam (100% water vapor) at 600 and 800 °C, which is similar to industrial condition. Then we demonstrate that in steam of 600 °C, SBA-15 materials show very good hydrothermal stability and the materials with thicker walls and more micropores possess better stability. The structures of SBA-15 materials are easily destroyed under steam of 800 °C. High-temperature thermal treatment is proved to be an effective method to increase the polymerization degree and improve the hydrothermal stability. Nevertheless it will cause severe shrinkage of the mesopores. Herein, we demonstrate a carbon-propping approach to dramatically increase the hydrothermal stability of SBA-15 under such critical condition, in pure steam of 800 °C for 12 h.

Experimental Section

1. Chemicals. Triblock poly(ethylene oxide)-*b*-poly(propylene oxide)-*b*-poly(ethylene oxide) copolymer Pluronic P123 (MW = 5800, $EO_{20}PO_{70}EO_{20}$) was bought from Aldrich Chemical Inc. Other chemicals were purchased from Shanghai Chemical Co. All chemicals were used as received without further purification. Millipore water was used in all experiments.

2. Synthesis. To investigate the effect of pore wall structures on the hydrothermal stability, five SBA-15 samples with different structure parameters were synthesized by varying the synthetic strategies.

S-1, S-2, and S-3 samples were synthesized by the following procedure: 4.0 g of P123 was dissolved in 30 mL of water and 120 mL of a 2 M HCl solution. Then 8.4 g of TEOS (tetraethyl orthosilicate) was added, and the mixture was aged at 38 °C with stirring for 20 h. The mixture was then aged at 100, 70, and 120 °C for 24 h, respectively, corresponding to S-1, S-2, and S-3. The white solid products were collected by filtration, dried in air at room temperature, and then calcined at 550 °C in air for 5 h to remove the organic template.

The S-4 sample was prepared by the following method: 4.0 g of P123 and 8.0 g of KCl were dissolved in 30 mL of water and 120 mL of a 2 M HCl solution. Then 8.4 g of TEOS was added, and the mixture was aged at 38 °C with stirring for 20 h. The mixture was then aged at 100 °C for 24 h. The solid products of S-4 were collected by filtration, dried in air at room temperature, and then calcined at 550 °C in air for 5 h to remove the organic template. S-5 and S-6 samples were obtained by calcining S-1 in air at 750 and 900 °C for 6 h, respectively.

The S-7 sample was prepared by employing a carbon-propping method. First, mesostructured carbon−silica composites were prepared by impregnating glucose into the pores of S-1 according a previously reported method.[36] Then the composites were heated to 900 °C and maintained at 900 °C for 6 h under a nitrogen flow of 20 mL/min for carbonization. Finally, the carbonized composites were calcined at 750 °C in oxygen flow to remove carbon, and S-7 was obtained.

3. Hydrothermal Stability Evaluation. The investigation of the hydrothermal stability was performed by exposing the samples to pure steam (100% water vapor) at 600 or 800 °C at autogenous pressure for 3, 6, 12, and 24 h.

4. Characterization. Small-angle powder X-ray diffraction (XRD) patterns were recorded with a Bruker D4 powder X-ray diffractometer using Cu Kα radiation. Nitrogen adsorption−desorption isotherms were measured with a Micromeritics Tristar 3000 analyzer at 77 K. Before the measurements, the samples were outgassed at 200 °C in vacuum for 6 h. The Brumauer−Emmett−Teller (BET) method was utilized to calculate the specific surface areas. The pore volume and pore size distributions were derived from the adsorption branches of the isotherms using the Barrett−Joyner−Halanda (BJH) method. The total pore volume, V_p, was estimated from the amount adsorbed at a relative pressure of 0.95. The micropore volume (V_m) and micropore surface area were calculated by using the $V-t$ plot method. The t values were calculated as a function of the relative pressure using the de Boer equation, $t/\text{Å} = [13.99/((\log(p_0/p) + 0.034)]^{1/2}$. V_m was calculated using the following equation, $V_m/\text{cm}^3 = 0.001547I$, where I represents the Y intercept in the $V-t$ plot. The unit cell parameters were calculated using the formula $a = 2d_{100}/\sqrt{3}$, where d_{100} represents the d-spacing value of the (100) diffraction peak in XRD patterns of samples. The pore wall thickness was calculated from the following formula: $b = a - d$, where a represents the unit cell and d represents the pore diameter calculated using the BJH method. ^{29}Si solid-state NMR (nuclear magnetic resonance) experiments were performed on a Bruker DSX300 spectrometer with a frequency of 59.63 MHz, a recycling delay of 600 s, a radiation frequency intensity of 62.5 kHz, and the reference sample of Q8M8 ($[(CH_3)_3SiO]_8Si_8O_{12}$). Transmission electron microscopy (TEM) experiments were conducted on a JEOL 2011 microscope operated at 200 kV.

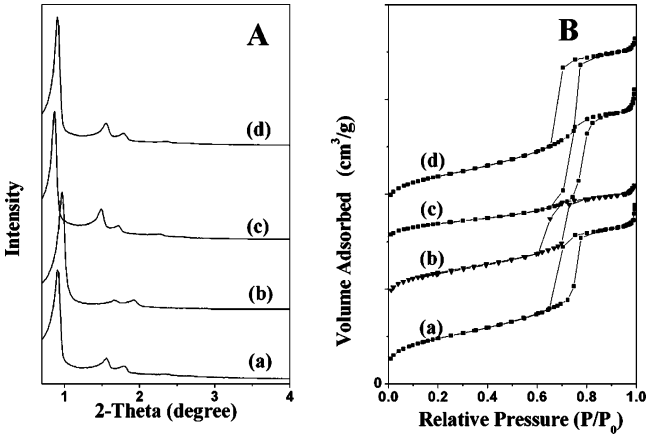

Figure 1. Powder XRD patterns (A) and N_2 adsorption−desorption isotherms (B) of samples S-1 (a), S-2 (b), S-3 (c), and S-4 (d). For clarity, the XRD patterns and the isotherms of b−d are offset on the *y*-axis.

TABLE 1: Unit Cell Parameter (*a*), Pore Diameter (*d*), Pore Wall Thickness (*b*), Pore Volume (V_p), BET Surface Area (S_{BET}), and Micropore Volume (V_m) of the Mesoporous Silica SBA-15 Materials

samples	*a* (nm)	*d* (nm)	*b* (nm)	V_p(cm^3/g)	S_{BET}(m^2/g)	V_m(cm^3/g)
S-1	11.3	9.0	2.3	1.17	690	0.03
S-2	10.6	7.3	3.3	0.81	603	0.05
S-3	11.7	10.0	1.7	1.03	365	0.01
S-4	11.3	9.6	1.7	1.17	635	0.01
S-5	10.0	7.4	2.6	0.55	380	0.01
S-6	9.5	6.0	3.5	0.45	310	0
S-7	10.0	6.9	3.1	0.51	360	0

Results and Discussion

1. Hydrothermal Stability of SBA-15 under Pure Steam of 600 °C. As reported, the pore parameters (pore size, wall thickness, and specific surface area, etc.) of SBA-15 may be well-controlled by varying the postsynthesis temperature and addition of inorganic salt during the synthesis.[3,7,37] Herein, four SBA-15 samples with different structural parameters, designated as S-1, S-2, S-3, and S-4, are synthesized. The powder XRD patterns and N_2 adsorption−desorption isotherms of the four samples are shown in Figure 1. These materials possess highly ordered two-dimensional (2-D) hexagonal mesostructures with uniform cylindrical channels. The structural parameters of these samples are listed in Table 1. It can be seen that each sample has distinct structural parameters. The distinct structural parameters may be helpful for better understanding the factors that affect the hydrothermal stability of SBA-15 materials. To evaluate the hydrothermal stability, these materials were treated with steam at 600 °C for 3, 6, 12, and 24 h.

Figure 2 shows XRD patterns and N_2 adsorption−desorption isotherms of S-1 before and after being treated with steam of 600 °C for 3, 6, 12, and 24 h. After steam treatment of 3 h, the (100) diffraction peak of sample S-1 shifts to larger 2θ degree and the relative intensity of diffraction peaks decreases, resulting in the disappearance of the (300) diffraction peak. The capillary condensation steps in N_2 sorption isotherms move to lower relative pressure range and the height of it decreased, suggesting smaller pore diameter and pore volume. The results suggest that the hydrothermal treatment may cause somewhat shrinkage of mesopores and structural disorder. Nevertheless, sample S-1 still displays three strong and well-resolved peaks, indexed as (100), (110), and (200) diffraction peaks of *P*6*mm* symmetry, suggesting a highly ordered mesostructure. The N_2 adsorption−desorption isotherms are still type IV curves with sharp and high capillary condensation steps, which are typical features of highly ordered *P*6*mm* mesostructures. When the hydrothermal treatment is prolonged to 6, 12, and 24 h, the change of XRD patterns and N_2 adsorption curves are very slight, as shown in Figure 2. The hexagonal mesostructure of S-1 is well-preserved even after the steam treatment at 600 °C for 24 h.

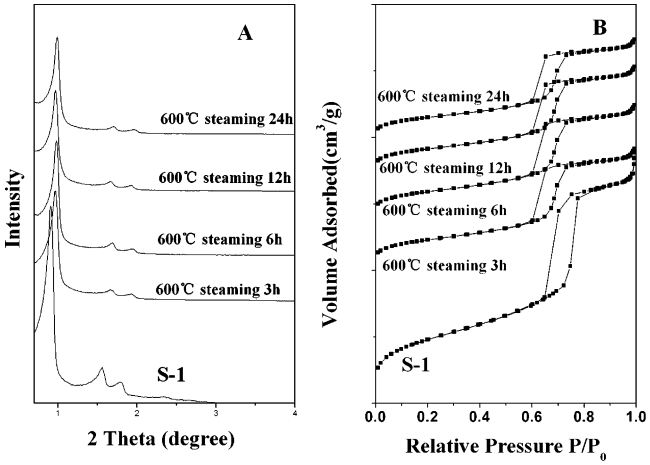

Figure 2. XRD patterns (A) and N_2 adsorption−desorption isotherms (B) of sample S-1 before and after being treated with steam of 600 °C for 3, 6, 12, and 24 h. For clarity, the XRD patterns and the isotherms are offset on the *y*-axis.

TABLE 2: Unit Cell Parameter (*a*), Pore Diameter (*d*), Pore Wall Thickness (*b*), Pore Volume (V_p), BET Surface Area (S_{BET}), and Micropore Volume (V_m) of S-1 after Steam Treatment at 600 °C of 3, 6, 12, and 24 h and S-2 to S-4 after Steam Treatment at 600 °C at 3 h

samples (steaming time)	*a* (nm)	*d* (nm)	*b* (nm)	V_p(cm^3/g)	S_{BET}(m^2/g)	V_m(cm^3/g)
S-1	11.3	9.0	2.3	1.17	690	0.03
S-1(3h)	10.5	6.5	4.0	0.55	299	0.006
S-1(6h)	10.5	6.5.	4.0	0.54	285	0.002
S-1(12h)	10.5	6.5	4.0	0.53	275	0.002
S-1(24h)	10.4	6.3	4.1	0.50	260	0.001
S-2	10.6	7.3	3.3	0.81	603	0.05
S-2(3h)	9.7	5.8	3.9	0.41	250	0.008
S-3	11.7	10.0	1.7	1.03	365	0.01
S-3(3h)	10.9	8.0[a]	2.9	0.71	285	0.002
S-4	11.3	9.6	1.7	1.17	635	0.01
S-4(3h)	10.3	7.5[a]	2.8	0.65	262	0.0015

[a] The pore size distributions of the samples became relatively wider after the steam treatment.

Table 2 lists the cell parameter, BET surface area, micropore volume, pore size, and pore wall thickness of sample S-1 before and after being treated with steam of 600 °C for 3, 6, 12, and 24 h. The cell parameter, BET surface area, pore size, and pore volume of S-1 decrease dramatically after the steam treatment of 3 h and change slightly when the hydrothermal treatment is prolonged to 6, 12, and 24 h. Unlike other structural parameters that decrease after hydrothermal treatment, the pore wall thickness of S-1 increases after the steam treatment of 3 h and changes only slightly when this treatment is prolonged. It is clear that the mesostructured silica materials become more robust and stable after being treated for 3 h. The ^{29}Si solid-state NMR spectra of S-1 before and after being treated with steam at 600 °C for 3 h are shown in Figure 3. Two bands, associated with Q^4 and Q^3 Si species, respectively, are observed for sample S-1 before the treatment. After the steam treatment of 3 h, only one main band associated with Q^4 Si species can

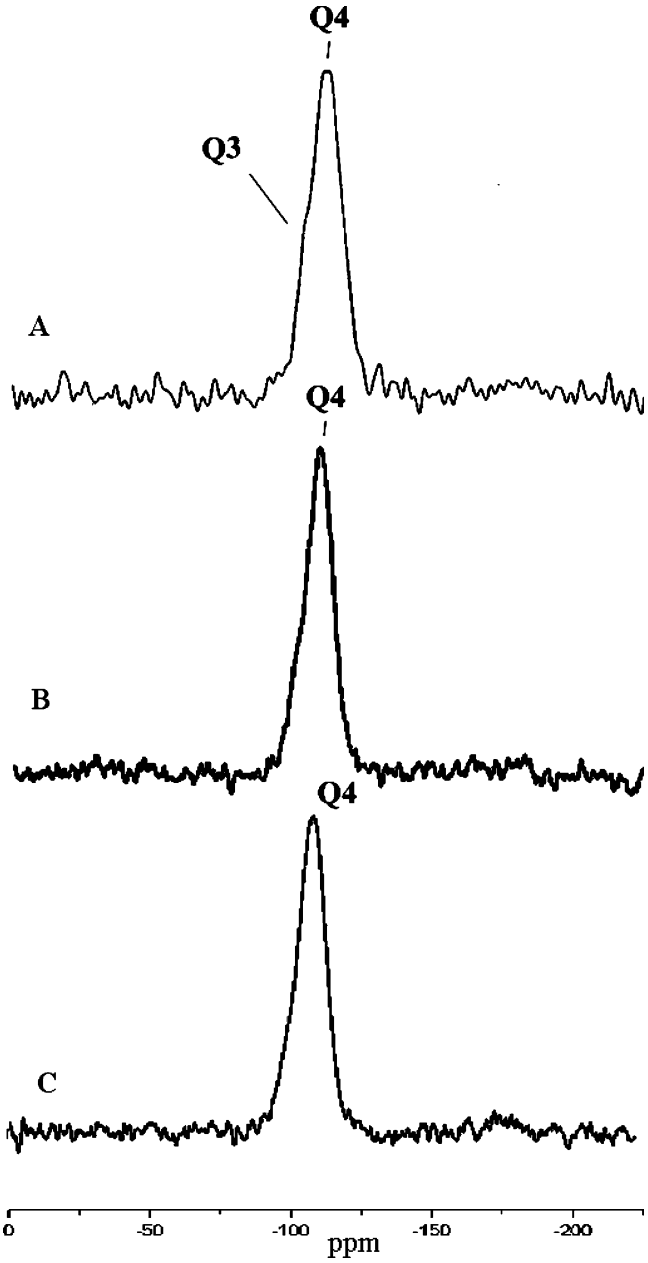

Figure 3. ^{29}Si solid-state NMR spectra of sample S-1 before (A) and after being treated with steam at 600 (B) and 800 °C (C) for 3 h.

be seen in the spectra, indicating that most of the silanols of sample S-1 dehydrolyze to ≡Si−O−Si≡ bonds and the polymerization degree is largely increased. The results further confirm that the silica walls become thicker and more robust. S-2, S-3, and S-4 samples also show good hydrothermal stability in steam of 600 °C, similar to that of sample S-1.

TEM images show that sample S-1 before the treatment has highly ordered mesostructures (Figure 4A), and after being treated with steam of 600 °C for 3 h the mesostructural regularity is well-retained (Figure 4B). By carefully comparing the TEM images of S-1 before and after the hydrothermal treatment, it can be clearly seen that the silica walls were thickened and the pore diameter decreased after the steam treatment, which are very well consistent with the results from N_2 sorption measurements.

The *V*−t plots of sample S-1 before and after being treated with steam at 600 °C for 3 h are shown in Figure 5. The micropore volume of these samples are derived from the following equation, $V_m/cm^3 = 0.001547I$, where *I* represents the

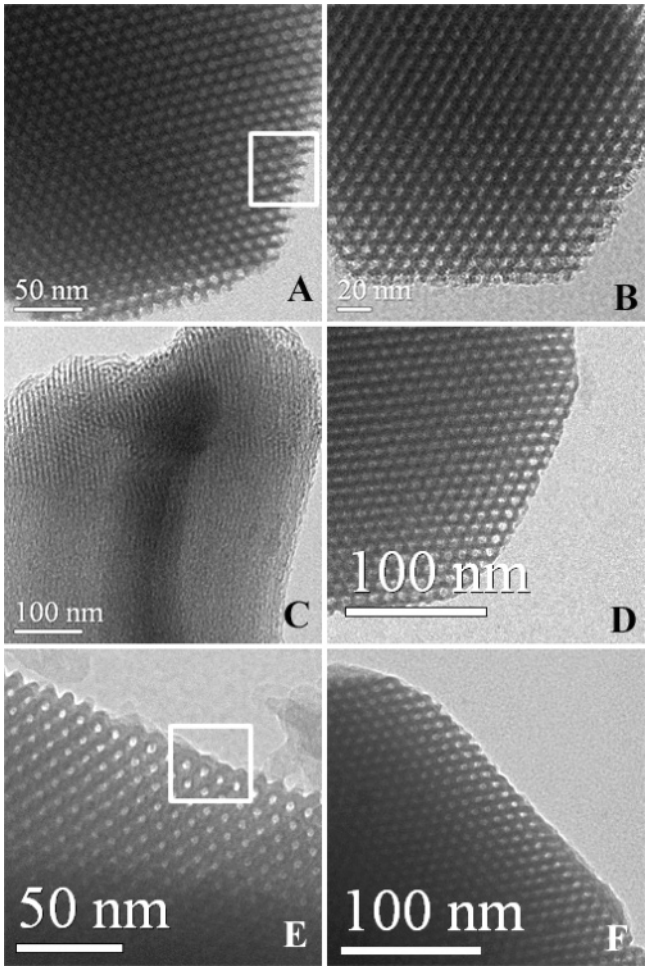

Figure 4. TEM images of samples before and after hydrothermal treatment: (A) sample S-1; (B) sample S-1 after the steam treatment of 3 h at 600 °C; (C) sample S-1 after the steam treatment at 800 °C for 3 h; (D) sample S-6; (E) sample S-6 after the steam treatment of 3 h at 800 °C; (F) sample S-7 after the steam treatment of 3 h at 800 °C.

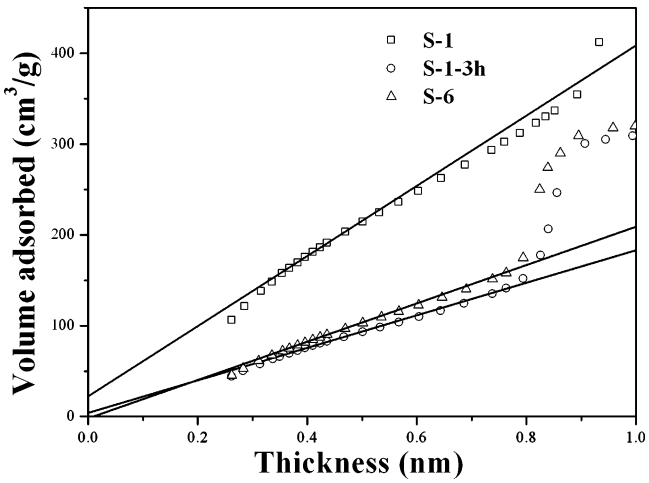

Figure 5. *V*−*t* plots of samples S-1, S-1(3h) (S-1 after hydrothermal treatment at 600 °C for 3 h), and S-6.

Y intercept of in the *V*−t plot. The micropore volumes of S-1, S-7, and S-1(3h) (S-1 after hydrothermal treatment at 600 °C for 3 h) are 0.03, 0.006, and 0, respectively. The as-synthesized SBA-15 materials contain both mesopores and micropores. The micropore volumes of all the samples are derived from the same method as shown above. After hydrothermal treatment, most of the micropores disappear.

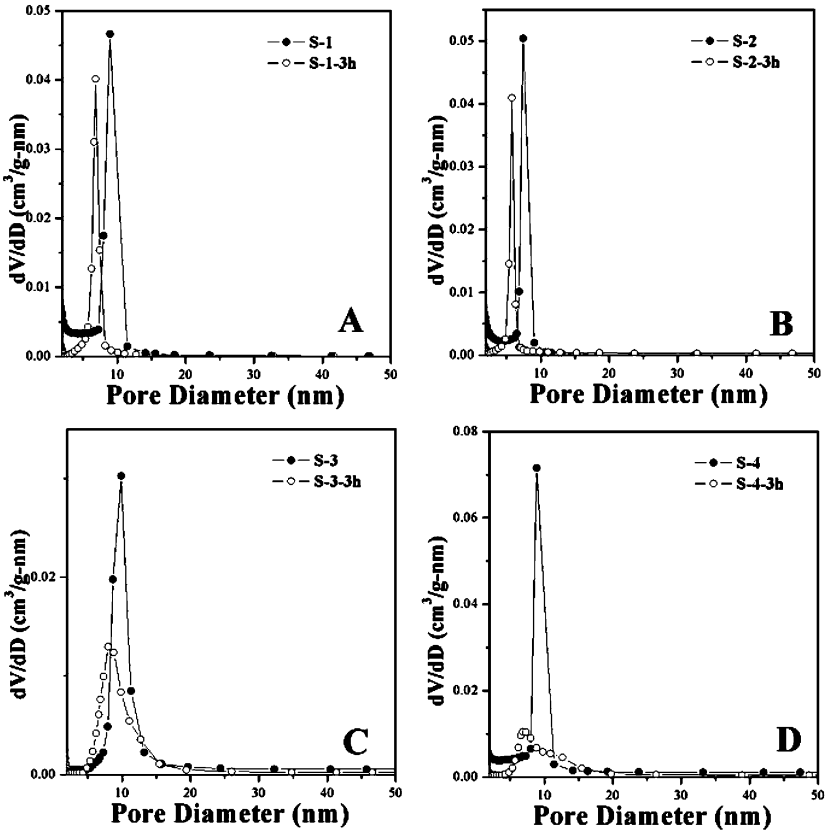

Figure 6. Pore size distribution curves of samples S-1 and S-1(3h) (A), S-2 and S-2(3h) (B), S-3 and S-3(3h) (C) and S-4 and S-4(3h) (D).

For further investigation of the effect of structural parameters on the hydrothermal stability of SBA-15, the cell parameters, pore diameters, pore wall thickness, BET surface areas, pore volumes, and micropore volumes of the four samples after the steam treatment of 3 h at 600 °C are listed in Table 2 for comparison. After the treatment, ~80% of the specific surface area for sample S-3 remains, whereas, >50% of the surface areas of samples S-1, S-2, and S-4 decrease. As illustrated in Table 2, most of the micropores on the silica wall disappear after steam treatment of 3 h at 600 °C. For SBA-15 materials, a considerable amount of mesopores are also contained in the pore wall,[32,33] which is illustrated from the pore size distribution curves shown in Figure 6. It can be seen from Figure 6 that the mesopores addressed in the pore wall also collapse greatly after the hydrothermal treatment. Both mesopores and micropores in the pore wall of SBA-15 materials collapse during the hydrothermal treatment. The decrease of the specific surface area is mainly caused by the collapse of the micropores and mesopores on the silica wall. For the mesostructured materials with more micropores and mesopores, such as S-1, S-2, and S-4, most of the micropores and mesopores in the pore wall collapse and the specific surface area decreases greatly. The pore volume of micropore and mesopores in the pore wall of sample S-3 is much smaller than that of other samples due to the higher postsynthesis treatment temperature. Therefore, the decrease of the surface area is slighter than that of other samples.

N_2 sorption isotherms of the four samples before and after the steam treatment at 600 °C are all type IV curves with type H_1 hysteresis loops. The capillary condensation steps in the isotherms of S-3 and S-4 after the treatment are much wider compared to those of S-1 and S-2. It can be seen from Figure 6 that after the steam treatment, the pore size distributions of S-1 and S-2 are still very narrow, whereas those of S-3 and S-4 become much wider, suggesting relatively poorer mesostructural regularity of S-3 and S-4. It can be concluded that the hydrothermal stability of samples S-1 and S-2 is relatively better than that for S-3 and S-4. The specific surface area, pore size, wall thickness, and micropore volume of samples S-1 to S-4 are shown in Figure 7 via use of a column scheme for better illustration of the influence of structural parameters on the hydrothermal stability. It may be concluded from Figure 7 and Table 2 that the mesostructured materials with larger micropore volume and thicker pore walls may have better hydrothermal stability under steam at 600 °C.

High-temperature steam can cause the shrinkage and even the complete destruction of the mesopores. It was previously reported that boiling water may cause the hydrolysis of ≡Si−O−Si≡ linkages and increase the amount of Q^3 Si species.[28,38] The collapse of mesoporous silica materials is mainly attributed to the continuous hydrolysis of ≡Si−O−Si≡ bonds. Nevertheless, the effect of high-temperature steam is quite different from that of boiling water. The high-temperature steam can cause the hydrolysis of ≡Si−O−Si≡ bonds to ≡Si−OH bonds on the surface of amorphous walls of mesoporous silica. The ≡Si−OH bonds may further cross-link and dehydrolyze to ≡Si−O−Si≡ bonds at the same time due to the high-temperature thermal treatment,[28,39] and the latter process is dominating. It was proved by the ^{29}Si solid-state NMR spectra that the Q^3 Si species are decreased after the steam treatment. As shown in Scheme 1, the hydrolysis and dehydrolysis reactions can cause the recombination of Si−O−Si on the amorphous silica walls of SBA-15, especially on the surface of the micropores, where numerous silanols are located. As a result, the polymerization degree is largely increased. The structural destruction should be attributed to the recombination effect of the steam at high temperature. Under steam at 600 °C, the mesostructures of SBA-15 samples collapse greatly in the first 3 h due to the structural recombination and as a result the polymerization

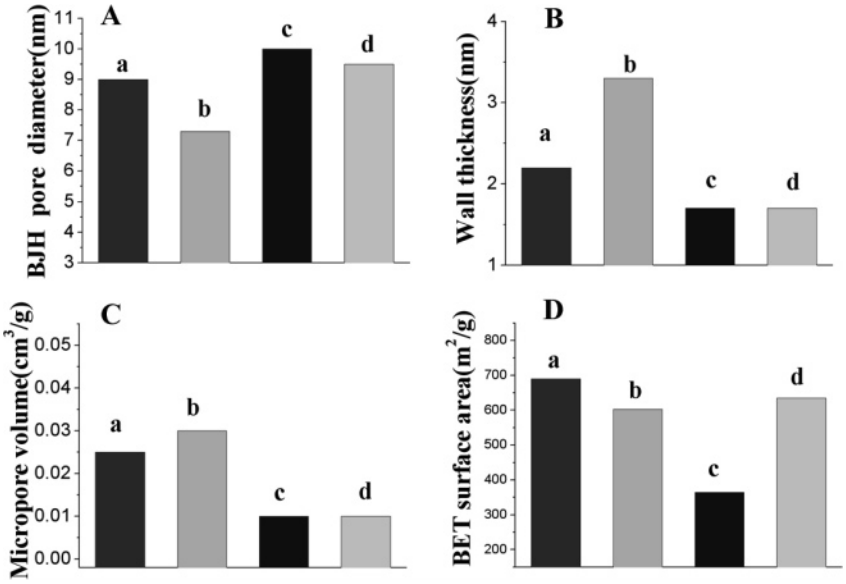

Figure 7. The column scheme of pore diameter (A), pore wall thickness (B), micropore volume (C), and specific surface area (D) of samples S-1 to S-4 (a−d).

SCHEME 1: Recombination Effect of Steam at High Temperature on the Pore Wall Structures of SBA-15 Materials

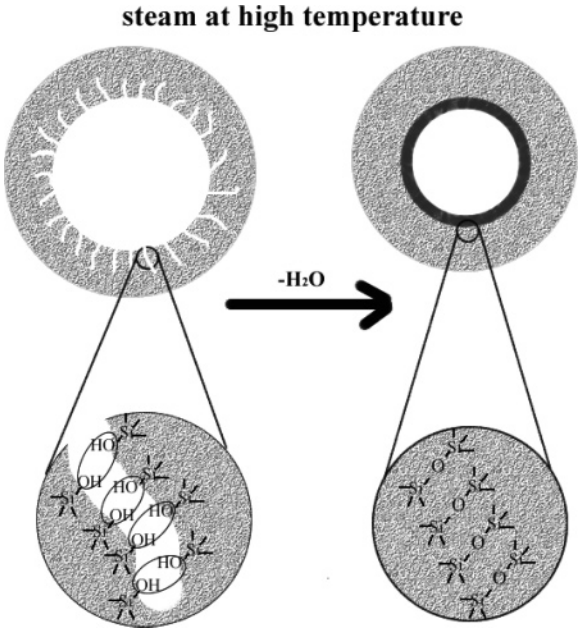

degree of Si−O−Si linkages is greatly enhanced. When the hydrothermal treatment is prolonged, few structural recombinations occur and the structure changes only slightly. Thus, these materials display excellent hydrothermal stability under steam at 600 °C.

There are many micropores on the pore walls of silica SBA-15 materials. For the materials with more micropores and thicker walls, the Si−O−Si linkages in the micropores are easily recombined under steam at 600 °C, as shown in Scheme 1. Such recombination takes place primarily around the micropore in the walls and may not severely destroy the pore wall structure, and the long-range order of the mesostructure is well-preserved after the hydrothermal treatment. For the mesostructured materials with fewer micropores and thinner walls, the recombination process would cause direct destruction to the pore walls. Therefore, the SBA-15 materials with thicker walls and more micropores may possess better long-range order after hydrothermal treatment and show relatively better hydrothermal stability.

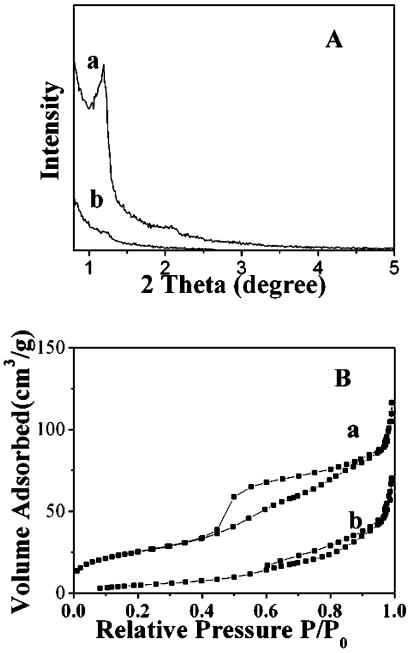

Figure 8. XRD patterns (A) and N_2 adsorption−desorption isotherms (B) of sample S-1 after treatment with steam at 800 °C for 3 (a) and 6 h (b).

2. Hydrothermal Stability of SBA-15 under Pure Steam at 800 °C. XRD patterns and N_2 adsorption−desorption isotherms of sample S-1 before and after treatment at 800 °C are shown in Figure 8. After being treated with the steam at 800 °C for 3 h, sample S-1 displays only one low-intensity diffraction peak in XRD patterns. When the treatment is prolonged to 6 h, no diffraction peak can be observed any more. After hydrothermal treating under such a severe condition for 3 h, the N_2 sorption isotherms are no longer the typical curves of *P6mm* mesostructures. The specific surface decreased greatly from ∼700 to <100 m^2/g, and the pore volume, from ∼1.1 to ∼0.2 cm^3/g, suggesting that the mesostructures are seriously

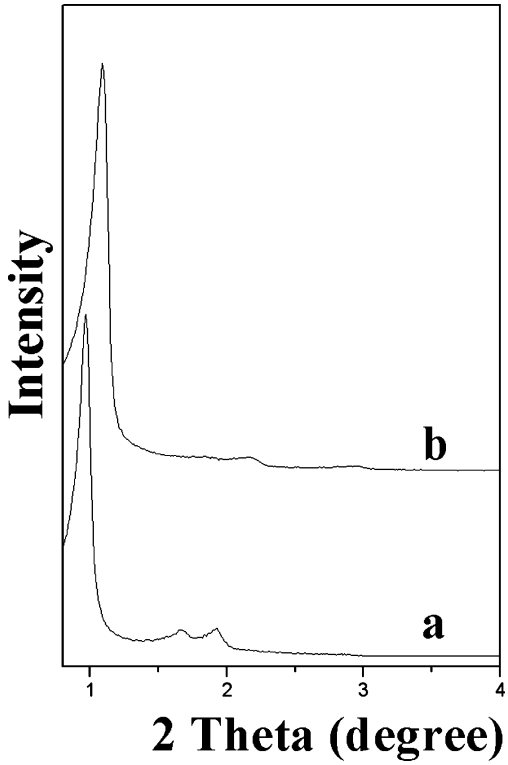

Figure 9. XRD patterns of samples S-5 (a) and S-6 (b). Pattern b is offset on the *y*-axis for clarity.

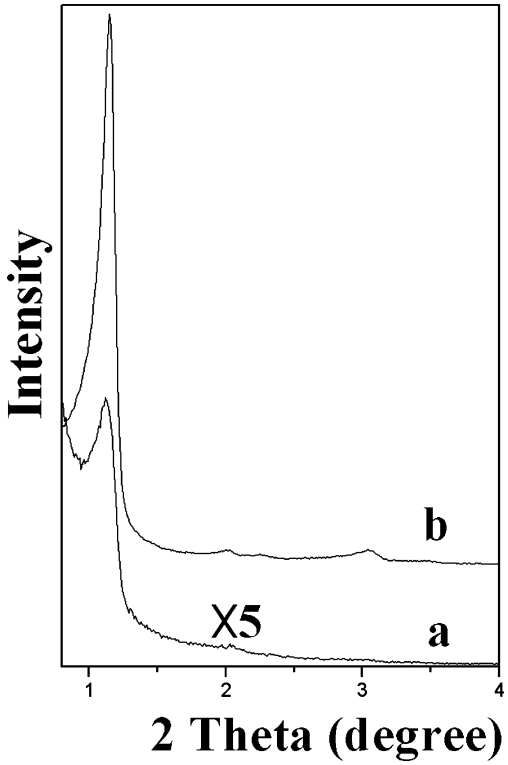

Figure 10. XRD patterns of mesoporous silica S-5 (a) and S-6 (b) treated with steam at 800 °C for 3 h. The pattern of sample S-5 is magnified 5 times for clarity.

destroyed. After treating for 6 h, no capillary sorption step can be observed over the relative pressure range $0.2 < P/P_0 < 0.8$, suggesting that no mesopores are preserved.

The TEM image of S-1 treated with steam at 800 °C for 3 h (Figure 4C) shows poor ordered structures, again suggesting the serious structure collapse of sample S-1 under such severe conditions. The ^{29}Si solid-state NMR spectrum of S-1 after the steam treatment of 3 h at 800 °C is shown in Figure 3C. It can be seen that almost all of the Q^3 Si species of sample S-1 dehydrolyze to Q^4 Si species after the treatment, indicating a higher polymerization degree. Similarly, S-2 to S-4 samples also show poor hydrothermal stabilities under steam at 800 °C.

Commonly, mesostructured silica materials are obtained after calcinations at 550 °C. We calcined S-1 at higher temperatures of 750 and 900 °C to obtain samples S-5 and S-6, respectively. XRD patterns of S-5 and S-6 (Figure 9) show four well-resolved diffraction peaks associated with (100), (110), (200), and (300) reflections of *P6mm* symmetry, suggesting highly ordered mesostructures. To evaluate the hydrothermal stability, S-5 and S-6 were treated with pure steam at 800 °C for 3 h. The XRD patterns of S-5 and S-6 after this treatment are shown in Figure 10. Only one weak diffraction peak can be observed in the XRD patterns of S-5, suggesting that the hexagonal mesostructure is completely destroyed. For sample S-6, there are three well-resolved peaks in the XRD patterns after the treatment. The hexagonal *P6mm* mesostructure of S-6 is well-preserved after such a severe hydrothermal treatment. N_2 adsorption−desorption isotherms of S-5 and S-6 after the steam treatment are shown in Figure 11. The type IV isotherm curves of sample S-5 disappear, and the BET surface area surface area decreases to <100 m^2/g and the pore volume to 0.2 cm^3/g. The results suggest that, after such a severe hydrothermal treatment, the mesostructure of sample S-5 is badly destroyed, indicating a poor hydrothermal stability similar to S-1 under such conditions. Different from S-5, the XRD pattern (Figure 10) of S-6 still shows three well-resolved diffraction peaks of an ordered

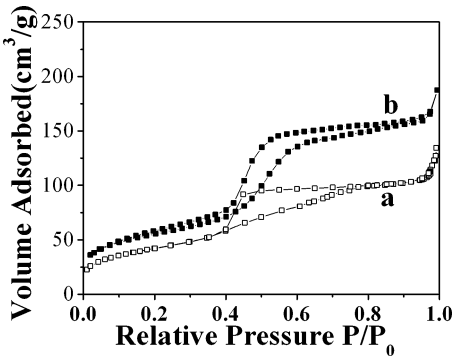

Figure 11. N_2 adsorption−desorption isotherms of mesoporous silica S-5 (a) and S-6 (b) treated with steam at 800 °C for 3 h.

hexagonal mesostructure. N_2 sorption isotherms of S-6 are still type IV curves with H_1 hysteresis loop after the treatment. The hexagonal mesostructure of S-6 is well-preserved, while the BET surface area decreases largely from ∼310 to ∼190 m^2/g and the pore volume to 0.3 cm^3/g. When the treatment is prolonged to 6 and 12 h, as shown in Table 3, the *d*-spacing value and the BET surface area of S-6 change only slightly, exhibiting very good hydrothermal stability. It is very similar to the one obtained after the hydrothermal treatment of S-1 under steam at 600 °C. After the steam treatment at 800 °C for 3 h, sample S-6 becomes a more stable one and further treatment just causes slight damage to the mesostructure.

TEM images of S-6 before and after steam treatment for 3 h at 800 °C are shown in Figure 4D,E, respectively. It can be seen that sample S-6 has smaller pores and thicker wall compared to sample S-1. After being treated with steam at 800 °C for 3 h, the *P6mm* structure of sample S-6 is well-preserved, the wall became much thicker, and the pore diameter decreases greatly, indicating good hydrothermal stability of sample S-6 under steam at 800 °C. Interestingly, looking at the edge of the

TABLE 3: Structural Parameters, Such as Unit Cell Parameter (*a*), Pore Diameter (*d*), Pore Wall Thickness (*b*), Pore Volumes (V_p), BET Surface Area (S_{BET}), and Micropore Volume (V_m), of Samples S-6 and S-7 before and after Being Treated with Steam at 800 °C for 3, 6, and 12 h

sample (steaming time)	*a* (nm)	*d* (nm)	*b* (nm)	V_p (cm^3/g)	S_{BET} (m^2/g)	V_m (cm^3/g)
S-6	9.5	6.0	3.5	0.45	310	0
S-6(3h)	9.0	4.1	4.9	0.30	196	0
S-6(6h)	9.0	4.1	4.9	0.29	190	0
S-6(12h)	9.0	4.1	4.9	0.28	185	0
S-7	10.0	6.9	3.1	0.51	360	0
S-7(3h)	9.3	5.1	4.2	0.40	255	0
S-7(6h)	9.3	5.1	4.2	0.38	240	0
S-7(12h)	9.3	5.1	4.2	0.36	230	0

images (Figure 4A,E), after the treatment, the silica walls on the boundary become smoother compared with those for sample S-1, further implying that a "minor" reorganization of the wall such as recombination of the Si−O−Si linkage occurs during the treatment.

It is clear that the hydrothermal stability for S-6 is better than that for S-1 and S-5. The calcining temperature has great influence on the hydrothermal stability of mesostructured silica SBA-15. The structure parameters of S-1, S-5, and S-6 are shown in Table 1. The wall thickness of S-1 was greatly increased when the calcining temperature was raised to 750 and 900 °C. The ^{29}Si solid-state NMR spectra of S-1 and S-6 are shown in Figure 12. Two bands, one main band associated with Q^4 Si species and one weak shoulder band associated with Q^3 Si species, can be observed for sample S-1. In contrast to S-1, only one main band associated with Q^4 Si species in the NMR spectra (Figure 12) is observed for sample S-6. After calcining at 900 °C for 3 h, the polymerization of ≡Si−O−Si≡ bonds is greatly enhanced and most of Q^3 Si species have disappeared.

High-temperature calcination is an effective method to enhance the hydrothermal stability of SBA-15 materials under such severe conditions. Under steam at 800 °C, the recombination of the Si−O−Si linkage is performed much more rapidly and severely compared to that under steam at 600 °C. Therefore, the structures of silica SBA-15 materials obtained after calcination at 550 and 750 °C are easily destroyed by the high-temperature steam. Calcination at 900 °C may largely increase the polymerization degree of the Si−O−Si linkages on the pore walls of SBA-15 materials,[40] as proved by the ^{29}Si solid-state NMR spectra. For the mesostructured materials with high polymerization degree, the recombination reactions under steam at 800 °C may be minimized and just cause slighter structural destruction. As a result, the long-range order of such materials can be well-preserved after the steam treatment. The recombination reactions under steam can increase the polymerization degree of such materials. Therefore, when the treatment is prolonged, few structural recombinations occur and the structure changes very slightly. The materials reveal very good hydrothermal stability under steam at 800 °C.

Nevertheless, the calcining procedure causes an undesirable shrinkage of the mesopores of SBA-15. After calcination at 900 °C, the pore diameter of S-1 decreased from 9.0 to 6.0 nm and the specific surface area from 690 to 300 m^2/g. To minimize the unexpected shrinkage of mesopores caused by the high-temperature calcination, a carbon-propping method is introduced to enhance the hydrothermal stability and minimize the shrinkage at the same time. First, mesostructured Si/C composites were synthesized following a procedure reported previously.[36] The composite materials were heated to 900 °C for 6 h under nitrogen, and then the carbon was removed by calcining at 750 °C in an air flow. The obtained materials were designated as S-7. The evaluation of the hydrothermal stability of S-7 was performed under pure steam at 800 °C for 3, 6, and 12 h. The XRD patterns and N_2 adsorption−desorption isotherms of S-7 before and after the hydrothermal treatment are shown in Figure 13. XRD patterns of S-7 before and after the treatment show four well-resolved diffraction peaks associated with (100), (110), (200), and (300) reflections of *P6mm* symmetry, indicating a highly ordered mesostructure. All of the N_2 adsorption−desorption isotherms for sample S-6 with the treatments are type IV curves with H_1 hysteresis loop. As shown in Figure 13, sample S-7 shows similar structure parameters after hydrothermal treatment for 3, 6, and 12 h, exhibiting very good hydrothermal stability. Compared to S-6, prepared via the direct high-temperature calcination at 900 °C, sample S-7 has relatively larger pore size, specific surface area, and pore volume, which benefit from the carbon-propping high-temperature treatment. As a result, after hydrothermal treatment for 3 h at 800 °C, S-7 displays larger pore diameter (5.1 nm), pore volume (0.4 cm^3/g), and specific surface area (255 m^2/g) (Table 3) compared to S-6 after the same treatment (with pore diameter of 4.1 nm, specific surface area of 190 m^2/g, and pore volume of 0.3 cm^3/g).

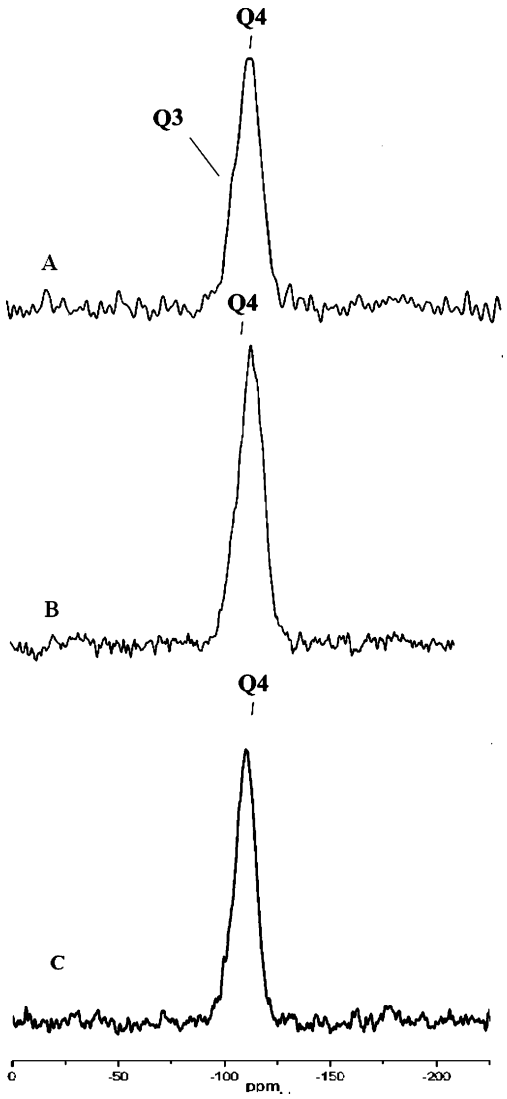

Figure 12. ^{29}Si solid-state NMR spectra of mesoporous silica S-1 (A), S-6 (B), and S-7 (C).

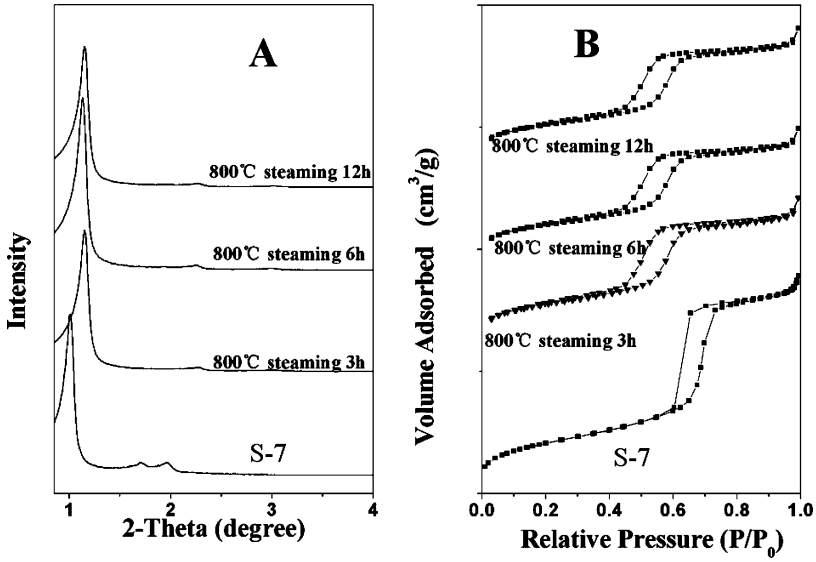

Figure 13. XRD patterns (A) and N_2 adsorption−desorption isotherms (B) of sample S-7 before and after steam treatment at 800 °C for 3, 6, and 12 h.

TEM images of S-6 and S-7 after being treated with steam at 800 °C for 3 h are shown in Figure 4E,F, respectively. After hydrothermal treatment at 800 °C, sample S-7 possesses larger pores and more ordered structures compared to sample S-6 after the treatment, indicating that sample S-7 has better hydrothermal stability under such a severe hydrothermal treatment, pure steam at 800 °C.

The carbon-propping high-temperature treatment is proved to be an effective method to enhance the hydrothermal stability of SBA-15. It can be explained by the fact that the carbon-propping method can increase the polymerization degree of ≡Si−O−Si≡ bonds and minimize the undesirable shrinkage of mesopores at the same time during the high-temperature-treatment procedure, because the mesopore channels are underpropped by the carbon rods.

Conclusions

Mesostructured silica materials SBA-15 show very good hydrothermal stability under steam at 600 °C. Under such conditions the mesostructure collapses largely during the first 3 h and then changes slightly when the treatment is prolonged. The recombination effect of the Si−O−Si linkages in the amorphous walls of mesostructured silica materials may largely increase the polymerization degree and enhance the hydrothermal stability. Thicker pore walls and more micropores will result in relatively better hydrothermal stability. Under more critical conditions, steam at 800 °C, the SBA-15 mesostructure is easily destroyed, due to the more rapid and severe recombination of Si−O−Si in the pore wall. The polymerization degree is the main factor that influences the hydrothermal stability of SBA-15 materials under steam at 800 °C. Two methods are introduced to improve the hydrothermal stability. Thermal treatment at 900 °C can enhance the polymerization degree and improve the hydrothermal stability under the critical condition at 800 °C. Nevertheless, an undesirable shrinkage of mesopores may occur at the same time. We first employed a carbon-propping, high-temperature thermal treatment approach to increase the polymerization and minimize the shrinkage during the treatment. The materials obtained following this approach show superior hydrothermal stability under such critical condition with pure steam at 800 °C.

Acknowledgment. This work was supported by the National Natural Science Foundation of China (Grants 20421303, 20233030), State Key Basic Research Program of PRC (Grants G200048001, 2002AA321010), Shanghai Science and Technology Committee (Grants 03DJ14004, 03527001), China National Petroleum Corp. Research Grant (Grant 040803-03-00), Shanghai HuaYi Chemical Group, and Fudan Graduate Innovation Funds.

References and Notes

(1) Kresge, C. T.; Leonowicz, M. E.; Roth, W. J.; Vartuli, J. C.; Beck, J. S. *Nature* **1992**, *359*, 710.
(2) Beck, J. S.; Vartuli, J. C.; Roth, W. J.; Leonowicz, M. E.; Kresge, C. T.; Schmitt, K. D.; Chu, C. T. W.; Olson, D. H.; Sheppard, E. W.; McCullen, S. B.; Higgins, J. B.; Schlenker, J. L. *J. Am. Chem. Soc.* **1992**, *114*, 10834.
(3) Zhao, D. Y.; Feng, J. L.; Huo, Q. S.; Melosh, N.; Fredrickson, G. H.; Chmelka, B. F.; Stucky, G. D. *Science* **1998**, *279*, 548.
(4) Zhao, D. Y.; Huo, Q. S.; Feng, J. L.; Chmelka, B. F.; Stucky, G. D. *J. Am. Chem. Soc.* **1998**, *120*, 6024.
(5) Bagshaw, S. A.; Prouzet, E.; Pinnavaia, T. J. *Science* **1995**, *269*, 1242.
(6) Liu, X. Y.; Tian, B. Z.; Yu, C. Z.; Gao, F.; Xie, S. H.; Tu, B.; Che, R. C.; Peng, L. M.; Zhao, D. Y. *Angew. Chem., Int. Ed.* **2002**, *41*, 3876.
(7) Yu, C. Z.; Tian, B. Z.; Fan, B.; Stucky, G. D.; Zhao, D. Y. *Chem. Commun.* **2001**, 2726.
(8) Tanev, P. T.; Pinnavaia, T. J. *Science* **1995**, *267*, 865.
(9) Tanev, P. T.; Chibwe, M.; Pinnavaia, T. J. *Nature* **1994**, *368*, 321.
(10) Ryoo, R.; Kim, J. M.; Ko, C. H.; Shin, C. H. *J. Phys. Chem.* **1996**, *100*, 17718.
(11) Luan, Z. H.; Maes, E. M.; van der Heide, P. A. W.; Zhao, D. Y.; Czernuszewicz, R. S.; Kevan, L. *Chem. Mater.* **1999**, *11*, 3680.
(12) Alba, M. D.; Luan, Z. H.; Klinowski, J. *J. Phys. Chem.* **1996**, *100*, 2178.
(13) Xu, J.; Luan, Z. H.; Hartmann, M.; Kevan, L. *Chem. Mater.* **1999**, *11*, 2928.
(14) Corma, A.; Navarro, M. T.; Pariente, J. P. *J. Chem. Soc., Chem. Commun.* **1994**, 147.
(15) Baltes, M.; Cassiers, K.; Van Der Voort, P.; Weckhuysen, B. M.; Schoonheydt, R. A.; Vansant, E. F. *J. Catal.* **2001**, *197*, 160.
(16) Trong-On, D.; Ungureanu, A.; Kaliaguine, S. *Phys. Chem. Chem. Phys.* **2003**, 5, 3534.
(17) Van Der Voort, P.; Baltes, M.; Vansant, E. F. *Cataly. Today* **2001**, *68*, 119.
(18) Kawi, S.; Shen, S. C. *Mater. Lett.* **2000**, *42*, 108.
(19) Ryoo, R.; Jun, S. *J. Phys. Chem. B* **1997**, *101*, 317.
(20) Ryoo, R.; Kim, J. M.; Ko, C. H. Mesoporous Molecular Sieves 1998, Proceedings of the International Symposium, 1st, Baltimore, MD. *Stud. Surf. Sci. Catal.* **1998**, *117*, 151.

(21) Kim, J. M.; Jun, S.; Ryoo, R. *J. Phys. Chem. B* **1999**, *103*, 6200.
(22) Mokaya, R. *J. Phys. Chem. B* **1999**, *103*, 10204.
(23) Mokaya, R.; Jones, W. *Chem. Commun.* **1998**, 1839.
(24) On, D. T.; Kaliaguine, S. *J. Am. Chem. Soc.* **2003**, *125*, 618
(25) Do, T. O., Nossov, A.; Springuel-Huet, M. A.; Schneider, C.; Bretherton, J. L.; Fyfe, C. A.; Kaliaguine, S. *J. Am. Chem. Soc.* **2004**, *126*, 14324.
(26) Jun, S.; Kim, J. M.; Ryoo, R.; Ahn, Y. S.; Han, M. H. *Microporous Mesoporous Mater.* **2000**, *41*, 119.
(27) Xia, Q. H.; Hidajat, K.; Kawi, S. *Mater. Lett.* **2000**, *42*, 102.
(28) Shen, S. C.; Kawi, S. *J. Phys. Chem. B* **1999**, *103*, 8870.
(29) Van Der Voort, P.; Baltes, M.; Vansant, E. F. *J. Phys. Chem. B* **1999**, *103*, 10102.
(30) Kruk, M.; Jaroniec, M.; Ko, C. H.; Ryoo, R. *Chem. Mater.* **2000**, *12*, 1961.
(31) Ryoo, R.; Ko, C. H.; Kruk, M.; Antochshuk, V.; Jaroniec, M. *J. Phys. Chem. B* **2000**, *104*, 11465.
(32) Joo. S. H.; Ryoo, R.; Kruk, M.; Jaroniec, M. *J. Phys. Chem. B* **2002**, *106*, 4640.
(33) Galarneau, A.; Cambon, N.; Di Renzo, F.; Ryoo, R.; Choi, M.; Fajula, F. *New J. Chem.* **2003**, *27*, 73.
(34) Newalkar, B. L.; Komarneni, S. *Chem. Mater.* **2001**, *13*, 4573.
(35) Liu, Y.; Pinnavaia, T. J. *Chem. Mater.* **2002**, *14*, 3.
(36) Jun, S.; Joo, S. H.; Ryoo, R.; Kruk, M.; Jaroniec, M.; Liu, Z.; Ohsuna, T.; Terasaki, O. *J. Am. Chem. Soc.* **2000**, *122*, 10712.
(37) Yu, C. Z.; Fan, J.; Tian, B. Z.; Zhao, D. Y.; Stucky, G. D. *Adv. Mater.* **2002**, *14*, 1742.
(38) Kim, J. M.; Ryoo, R. *Bull. Korean Chem. Soc.* **1996**, *17*, 66.
(39) Bermudez, V. M. *J. Phys. Chem.* **1970**, *74*, 4160.
(40) Ishikawa, T.; Matsuda, M.; Yasukawa, A.; Kandori, K.; Inagaki, S.; Fukushima, T.; Kondo, S. *J. Chem. Soc.*, Faraday Trans. **1996**, *92*, 1985.